ELSEVIER

Journal of Chromatography B, 753 (2001) 131–138

JOURNAL OF CHROMATOGRAPHY B

www.elsevier.com/locate/chromb

Study of the retention properties of warfarin enantiomers on a β-cyclodextrin polymeric support

Maïté Guillaume, Alain Jaulmes, Bernard Sébille, Nicole Thuaud, Claire Vidal-Madjar*

Laboratoire de Recherche sur les Polymères, CNRS-Université Paris 12 UMR C7581, 2 Rue Henry Dunant, 94320 Thiais, France

Abstract

High-performance liquid chromatography was used to study the retention properties of (*R*)- and (*S*)-warfarins on a silica support coated with a β-cyclodextrin polymer. The influence of the methanol content of the acetate buffer eluent was investigated at pH 4. The measure of the variations of retention time with temperature enables one to determine the enthalpy and the entropy of adsorption. The plot of the two thermodynamic functions shows a minimum around 30% (v/v) methanol. At low methanol contents, the decrease of the hydrophobic interactions with increasing methanol content explains the decrease of the enthalpic and entropic terms. Above 40% (v/v) methanol, the decrease of the adsorption enthalpy absolute value is due to the solvation by the organic component. From the analysis of peak shape in mass-overload conditions, the column capacity toward each enantiomer was determined. A lower capacity was found toward (*S*)-warfarin, the more retained enantiomer. Peak shape analysis in mass-overload conditions was used to determine the adsorption isotherm. A Langmuir-type adsorption isotherm accounts well for the experimental data.

Keywords: Enantiomer separation; β-Cyclodextrin polymeric support; Retention properties; Warfarin

1. Introduction

High-performance liquid chromatography (HPLC) using cyclodextrin (CD)-based chiral stationary phases is widely used for stereochemical analysis [1]. Many types of cyclodextrin stationary phases are now currently available as chemically bonded CDs [2,3] and CD polymers adsorbed on silica [4–7]. The solute's adsorption mechanism involves mainly hydrophobic interactions with the apolar cyclodextrin cavities, but other important factors contribute to chiral recognition as the hydrogen bonding between some polar groups of the molecules and the hydroxyl groups at the rim of the cyclodextrin moieties [1,8]. However, the separation mechanism is not fully understood, since the selectivity observed on the β-CD polymer differs from those observed on the chemically bonded supports. Other interactions may interfere and modify the selectivity of the support such as hydrogen bonding and Van der Waals interactions at the inlet of the cyclodextrin cavities or modification of the spatial arrangement of water molecules inside the cavities [9].

It has been shown that the chiral recognition differs according to the CD substitutant [10–12]. For instance, warfarin enantiomers are well separated on the hydroxypropyl-substituted CD (Cyclobond I RSP) [12] and on the epichlorhydrin–cyclodextrin polymer [5,6]. On other CD phases such as polyvinylimidazole–CD polymer [13] or chemically-bonded native β-CD (Cyclobond I) [14], warfarin enantiomers are not separated. In the present paper,

*Corresponding author.

0378-4347/01/$ – see front matter
PII: S0378-4347(00)00371-6

we study the retention properties of (*R*)- and (*S*)-warfarin, on the epichlorhydrin–β-CD polymer. With chromatographic experiments performed in the initial linear range of the equilibrium isotherm, i.e., at small solute sample sizes, information on the interaction energies will be obtained from the change in enthalpy and entropy of the solute transfer from dissolved to adsorbed state. In addition, for each enantiomer, overload effects will be examined from peak shape analysis to determine the adsorption isotherm and the column capacity.

2. Experimental

2.1. Materials

Racemic warfarin was from Aldrich (Milwaukee, WI, USA). The *R*-(+)- and *S*-(−)-warfarin enantiomers were purified by recrystallization according to the method of West et al. [15]. Chromatographic analysis shows that the purity for each enantiomer used is 99%. Epichlorhydrin was obtained from Prolabo (Fontenay-sous-Bois, France) and β-cyclodextrin from Orsan (Paris, France). The silica support (LiChrospher particle diameter 5 μm and pore size 100 Å) was purchased from Merck (Darmstadt, Germany).

2.2. Apparatus

The chromatographic system consists of a pump (HPLC Pump 420, Kontron Instruments, Zurich, Switzerland), a UV detector (Model SPD-6A, Shimadzu, Kyoto, Japan) set at 254 nm wavelength. An injector (Model 7125, Rheodyne, Berkeley, CA, USA) was used with a 20-μl sample loop.

2.3. Chromatographic method

The chromatographic packing was obtained by adsorption of a polycondensate of cyclodextrin and epichlorhydrin onto silica [16]. The polymer was then crosslinked with glutaraldehyde [17]. The silica support contains 16% (in mass) of polymer and 9.6% (in mass) of CD, or 0.087 mmol/g of support.

The chromatographic column (150×4.6 mm I.D.) was slurry-packed by Colochrom (Drancy, France), and the amount of support introduced in a column is 1.2 g. The amount of stationary phase per column is thus 0.115 g and contains 0.010 mmol of CD. From the partial molar volume of β-CD in solution (703.8 ml/mol, [18]), one can estimate the stationary phase volume, $V_s = 0.07$ ml.

The column temperature was maintained constant within ±0.1°C, using a thermostated water bath. The eluents used were obtained by varying the methanol content in a 0.1 *M* sodium acetate buffer (pH 4). The column dead volume ($V_m = 2.3$ ml) was determined from the elution time of the methanol peak.

2.4. Data acquisition system

The analog output of the detector was connected to a digital voltmeter (Model 199, Keithley, Cleveland, OH, USA) connected to a a personal computer (Compaq Deskpro, Model 386/20e, Houston, TX, USA).

2.5. Numerical simulation

A Fortran program was used to simulate the chromatographic process.

The numerical method used to solve the simplified differential equations of the solute progression along the column must render three main phenomena: the global dispersive effect, the mobile phase progression and the solute exchanges between the two phases.

(a) Dispersive effect: to modelize the dispersive effect, the column length is divided into an arbitrary number of slices, in which the equilibrium is assumed to be achieved at once. The thickness of the slices Δz is chosen so as to yield the same dispersive effect as estimated through the peak shapes. The band broadening of the elution peak (number of theoretical plates: 800) was numerically simulated by using 0.02 cm for the calculation step along the column length.

(b) Mobile phase progression: the mobile phase progression is rendered by a mere index shift after every time increment $\Delta t = \Delta z/u$.

(c) Solute exchanges: the method assumes that equilibrium is reached as soon as the new phase fractions meet in a given slice. Taking into account this assumption, the values $C(z-\Delta z, t)$ and $q(z, t)$

will originate the new values $C(z, t+\Delta t)$ and $q(z, t+\Delta t)$ obeying the mole balance equations. The initial values C_0 and q_0 give the total solute amount in the slice: $s=C_0+q_0$ which remains identical after the exchange: $s=C_e+q_e$ at equilibrium.

Using the isotherm equation: $q_e=f(C_e)$ (here the Langmuir isotherm, like in Eq. (6)), the root of the mole balance equation: $q_e+f(C_e)-s=0$, obtained by interpolation, will yield C_e and $q_e=f(C_e)$.

The method insures the solute conservation all through the percolation process.

One can use any isotherm.

One can approach the actual physicochemical phenomena as closely as desirable by choosing thinner slices.

The optimization of the parameters q_s and k' has been carried out by non-linear regression following the Simplex algorithm. Programming was performed in Fortran, using a personal computer (Optilex GX1 L500; Dell).

3. Results

In aqueous solutions warfarin is a weak acid, with $pK_a=4.8$ [19]. The retention of the two enantiomers and their enantioselectivity vary with the pH [4]. At low pH (pH 4) the chiral isomers are well separated and the (*S*) enantiomer is more retained. As shown in Fig. 1, for 20% methanol in the eluent, a good chiral discrimination is obtained ($\alpha=1.3$) with a baseline separation. The enantioselectivity is lower at higher pH and there is no more separation of warfarin enantiomers at pH 7. The variations of the retention thermodynamics with the methanol content in the eluent will be studied at pH 4. The elution behavior in mass-overload conditions was also examined to determine the adsorption isotherm.

3.1. Retention studies at infinite dilution

The logarithm of the capacity factor is found to be a linear function of the organic solvent composition, as shown in Fig. 2 for experiments carried out at 25°C, where the plot of ln k' vs. methanol volume fraction is given. The capacity factor k' for the solute at infinite elution is related to V_r, the retention

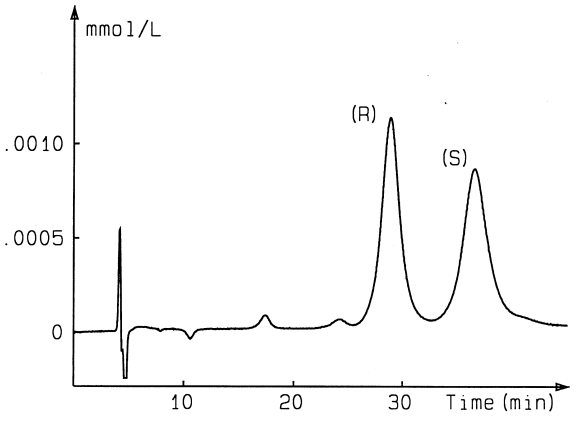

Fig. 1. Separation of warfarin enantiomers on a β-cyclodextrin polymeric column. Eluent: 20% methanol in 0.1 *M* sodium acetate buffer, at pH 4. Flow-rate: 0.5 ml/min; temperature: 25°C; sample loop: 20 μl; solute concentration: 10^{-4} mol/l.

volume extrapolated to zero sample size, and to *K*, the partition equilibrium constant:

$$k' = \frac{(V_r - V_m)}{V_m} = K\Phi \quad (1)$$

where *K* is the equilibrium constant, V_m is the mobile phase volume and $\Phi=V_s/V_m$. V_s is the volume of the stationary phase. With the polymeric stationary phase used, $\Phi=0.03$, as calculated from the value estimated for V_s.

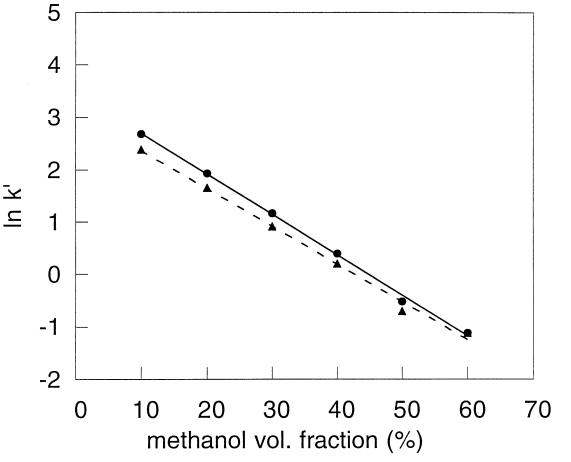

Fig. 2. Logarithm of capacity factor plotted versus methanol volume fraction. Experimental conditions as in Fig. 1. (●) (*S*)-Warfarin; (▲) (*R*)-warfarin.

The slope of the straight lines (Fig. 2) is slightly larger for the more retained (*S*)-warfarin enantiomer. Thus, as the volume fraction of methanol increases, the selectivity factor (α), equal to the k' ratio of (*S*)- to (*R*)-warfarin, decreases.

At infinite dilution, the standard Gibbs free energy ΔG^0 for the solute transfer from the dissolved to the adsorbed state is given by

$$\Delta G^0 = -RT \ln K = \Delta H^0 - T\Delta S^0 \quad (2)$$

where ΔH^0 and ΔS^0 are the corresponding standard enthalpy and entropy, respectively.

Combining Eqs. (1) and (2) gives for the capacity factor:

$$\ln k' = \frac{\Delta S^0}{R} + \ln \Phi - \frac{\Delta H^0}{RT} \quad (3)$$

The variation of ln k' with the reciprocal of the absolute temperature T yields a straight line (regression coefficient over 0.998), as shown in Fig. 3a, for various methanol contents in the buffer. From the linear van't Hoff plot, the retention thermodynamics (ΔH^0 and $\Delta S^0/R + \ln \Phi$) were, respectively, determined from the slope and the intercept at origin.

The variation of the thermodynamic retention data versus methanol composition are illustrated in Fig. 4. Both the enthalpic and the entropic terms are roughly parabolic functions of the methanol content, with a minimum between 30% and 40% (v/v) methanol.

The selectivity factor α is related to the corresponding thermodynamic quantities:

$$\ln \alpha = \frac{\Delta S^0_S - \Delta S^0_R}{R} - \frac{\Delta H^0_S - \Delta H^0_R}{RT} \quad (4)$$

where the subscripts S and R correspond, respectively to (*S*)- and (*R*)-warfarin. $\Delta(\Delta S^0)$ and $\Delta(\Delta H^0)$ will further represent the differences in the thermodynamic data of these enantiomers. Table 1 gives the values of α for different methanol contents at 25°C. The differences, $\Delta(\Delta S^0)$ and $\Delta(\Delta H^0)$, are also given in the same table.

At a given eluent composition, the variation of the selectivity factor with temperature results from the linear van't Hoff plot of each warfarin enantiomer. A linear relationship is thus obtained when ln α is plotted vs. $1/T$ (Fig. 3b) and the slopes of the straight lines are equal to $\Delta(\Delta H^0/R)$. The enantioselectivity decreases when increasing the methanol content in the eluent and for methanol volume fractions larger than 50%, warfarin enantiomers are no longer separated.

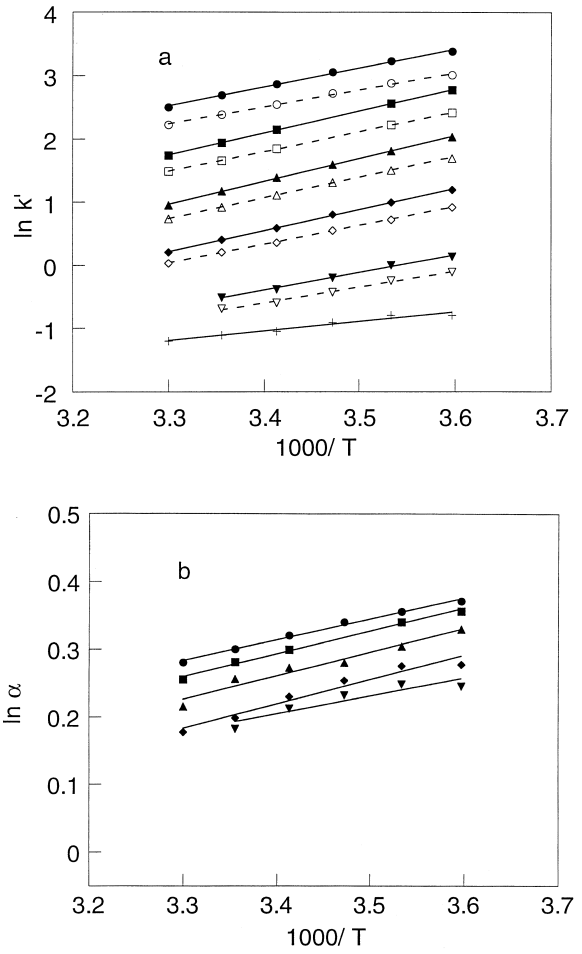

Fig. 3. Van't Hoff plot as a function of mobile phase composition. (a) k' plot, full and open symbols for, respectively, (*S*)- and (*R*)-warfarin. (b) Enantioselectivity plot. (●) 10%; (■) 20%; (▲) 30%; (♦) 40%; (▼) 50%; (+) 60% (v/v) methanol in 0.1 *M* acetate buffer.

3.2. Studies in mass-overload conditions

Studies in mass-overload conditions were performed for experiments carried out at 25°C, with an eluent containing 20% (v/v) methanol. The modification of peak shape as a function of the amount injected is illustrated in Fig. 5a and b. Because of the

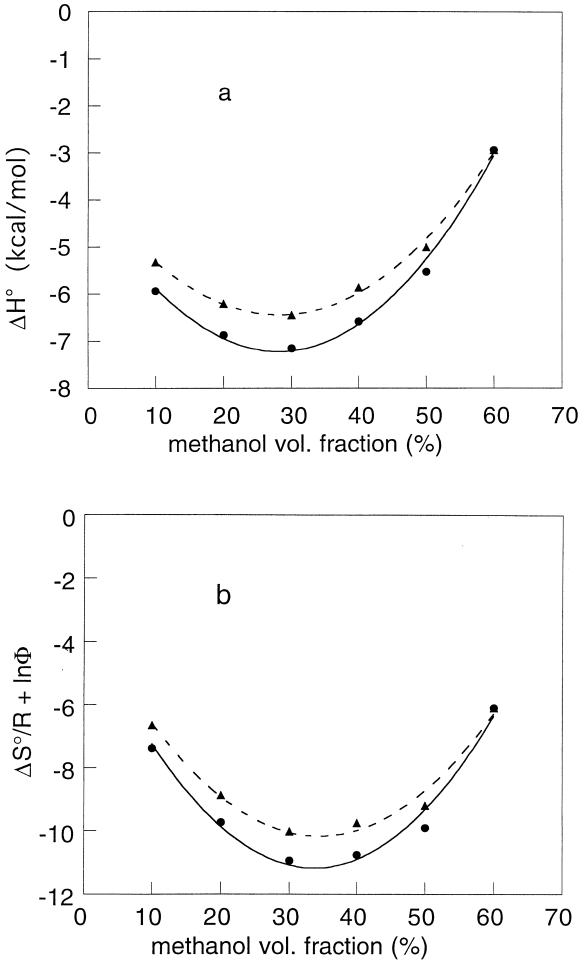

Fig. 4. Effect of methanol composition on the retention thermodynamics of warfarin enantiomers. (a) Adsorption enthalpy; (b) entropic term. (*R*)-Warfarin (▲) and (*S*)-warfarin (●) in mixtures of methanol + 0.1 *M* acetate buffer, at pH 4.

Table 1
Influence of methanol content on warfarin enantioselectivity at 25°C

Methanol content (%)	α	$\Delta(\Delta S^0)$ (cal/mol/°C)	$\Delta(\Delta H^0)$ (kcal/mol)	$\alpha_c = e^{-\Delta(\Delta H^0/RT)}$
10	1.33	−1.45	−0.6	2.8
20	1.33	−1.68	−0.7	3.3
30	1.29	−1.82	−0.7	3.3
40	1.23	−2.00	−0.7	3.3
50	1.20	−0.46	−0.5	2.3
60	1.00	0	0	1.00

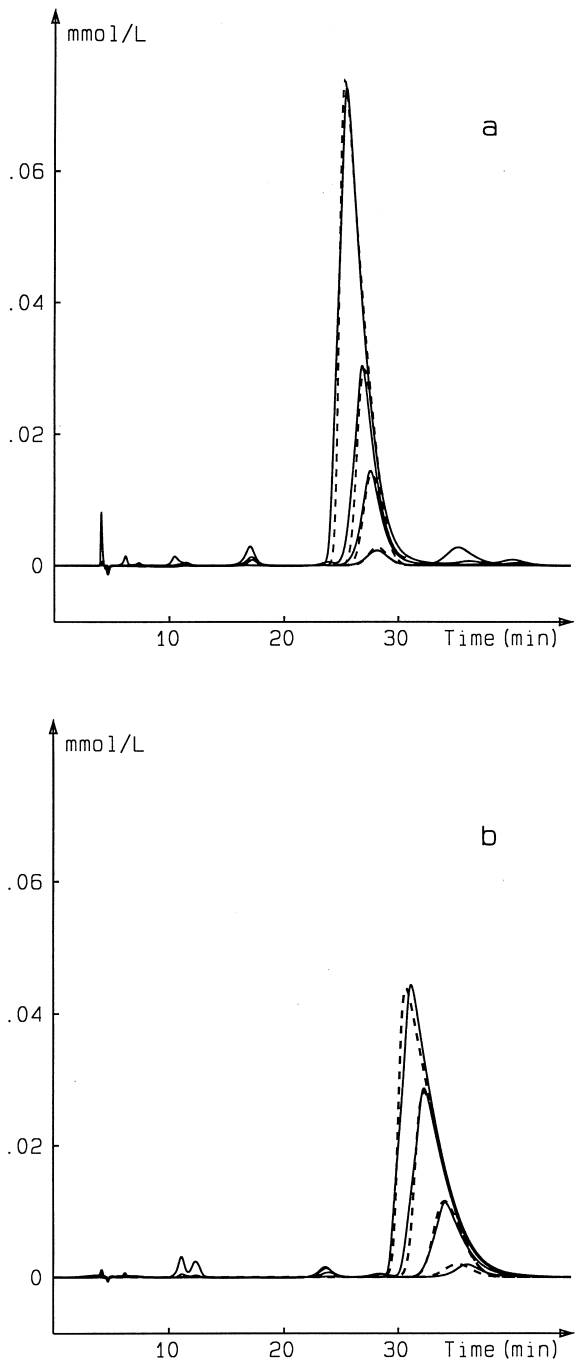

Fig. 5. Elution profiles of warfarin enantiomers in mass-overload conditions. (a) (*R*)-Warfarin; (b) (*S*)-warfarin. —— Experiment; ----- theoretical profile. Experimental conditions as in Fig. 1. Solute concentrations: 10^{-4}–$5\cdot10^{-3}$ mol/l.

limited range of the solute solubility, increasing amounts of the pure warfarin enantiomer were injected up to $5 \cdot 10^{-3}$ mol/l.

The adsorption isotherm was determined from the analysis of peak shapes observed in mass-overload conditions. The parameters defining the isotherm model were obtained by fitting the theoretical peak to the experimental one. The calculated profile results from a numerical simulation of the chromatographic process [20]. The method consists in solving the differential equation for solute migration:

$$\frac{\partial C}{\partial t} + u \cdot \frac{\partial C}{\partial z} + \frac{\partial q}{\partial t} = D' \cdot \frac{\partial^2 C}{\partial z^2} \quad (5)$$

where C is the solute concentration, q the amount of solute adsorbed per volume unit of mobile phase. z is the abscissa along the column length and t, the time elapsed from the moment of injection. u is the mobile phase velocity. D' is a global dispersion coefficient accounting for all the contributions to the dispersive effects.

In a previous paper we described a numerical method to account for dispersive effects [20] by including the band broadening in a global dispersion term. The simulation process, however, requires long calculation times. In this work, the dispersion was numerically simulated by defining a slice of thickness Δz, resulting in a band broadening as close as possible as that of the elution peak observed in linear elution conditions. In each slice the equilibrium is assumed to be reached with a solute mole balance kept constant.

The equilibrium between the mobile phase and the adsorbed phase is described by the adsorption isotherm. A simple form for a single-component adsorption isotherm is the Langmuir type isotherm with

$$q_a = q_s \frac{k'C}{q_s + k'C} \quad (6)$$

where q_a is the amount of solute adsorbed per unit of dead volume and q_s is the corresponding saturation capacity.

Within the concentration range studied, the theoretical profiles (dotted line) simulated on the basis of a Langmuir type isotherm fit well the experimental ones (solid line). The parameters q_s and k' (Table 2) were determined by fitting the simulated peaks to the experimental ones. A lower column capacity is found for the more retained enantiomer, with 3 mmol/l for (*S*)-warfarin and 5 mmol/l for (*R*)-warfarin. From studies in the range 20–40% (v/v) methanol, there was no significant variation of the column capacity. The difference in column capacities for the two enantiomers is clearly illustrated by comparing Fig. 5a and b, where the peak tailing for (*S*)-warfarin, at large amounts injected, is more important than that observed for (*R*)-warfarin.

Table 2
Parameters of the Langmuir adsorption isotherm (25°C)

Compound	Methanol content (%, v/v)	k'	q_s (mmol/l)
(*R*)-Warfarin	20	5.2	5.1
	30	2.6	4.9
	40	1.0	5.1
(*S*)-Warfarin	20	6.8	3.0
	30	3.2	3.4
	40	1.4	2.5

4. Discussion

As often observed in reversed-phase chromatography with methanol–water eluents [21,22], the retention volume decreases exponentially by increasing the content of methanol in the eluent (Fig. 2). The retention mechanism is however a complex one, as indicated from the variation of the adsorption enthalpy which becomes more negative as the methanol content increases from 10 to 30% (Fig. 4a). A similar diagram (Fig. 4b) is observed for the entropic term ($\Delta S^0/R + \ln \Phi$), since its value results from the sum of $\ln k'$ and $\Delta H^0/RT$. The adsorption enthalpy variations indicate a larger warfarin–stationary phase interaction energy around 30% (v/v) methanol in the eluent.

In the low organic solvent concentration range, the retention decrease with increasing methanol content is explained only by the important decrease of the ($\Delta S^0/R + \ln \Phi$) term because of important variations of the hydrophobic interactions. The change in the entropic term is then the major factor governing the variations of retention with the methanol content in the eluent. The lower ΔH^0 absolute value at 10%

(v/v) methanol is probably due to the expulsion of water molecules into the solvent during the adsorption process.

In contrast to this behavior, above 40% (v/v) methanol, the ΔH^0 absolute value decreases with increasing the organic solvent content. This result indicates a decrease of the interaction between warfarin and the stationary phase because of the solute solvation by the organic solvent [22]. Thus in this large methanol concentration range, the retention decrease is mainly due to the decrease of the absolute value of the enthalpic term.

For both enantiomers, parallel thermodynamic behaviors are observed with a retention resulting from a compensation between the enthalpic and entropic terms. In the 10–40% (v/v) methanol range, the difference $\Delta(\Delta H^0)$ in the adsorption enthalpies of warfarin enantiomers is between -0.6 and -0.7 kcal/mol (Table 1) and indicates a larger energy of interaction of (*S*)-warfarin with the β-CD polymer. A larger chiral discrimination is predicted from the energy difference with $\alpha_c = e^{-\Delta(\Delta H^0/RT)} \approx 3$. Instead, the observed separation factor α, is about 2.5-times as low and is continuously decreasing with increasing the methanol content in the eluent (Table 1). In fact, the mutual compensation between the enthalpic $\Delta(\Delta H^0)$ and entropic terms $\Delta(\Delta S^0)$ determines the difference in Gibbs free energy $\Delta(\Delta G^0)$ and thus the experimental separation factor. At methanol compositions larger than 40%, the important decrease of α value is explained by that of α_c, the chiral discrimination decreasing as the solute–stationary phase interaction energy is lower, because of warfarin solvation by the hydro–organic solvent.

Studies in overload conditions show that a Langmuir type isotherm model fits well the experimental profiles. The saturation capacities of the two enantiomers are different, about 40% lower for (*S*)-warfarin, the more retained enantiomer (Table 2). Larger saturation capacities for the less retained enantiomer have already been reported for the adsorption of (*R*)- and (*S*)-warfarin on immobilized human serum albumin [23].

The lower saturation capacity for (*S*)-warfarin may be explained by a lower number of binding sites because of the stronger steric conditions imposed by the formation of an inclusion complex of higher interaction energy inside the hydrophobic cyclodextrin cavities, in the particular environment of the polymeric structure. A comparison of the adsorption behavior of both enantiomers indicates that, in the 20–40% (v/v) methanol range, a lower number of stronger energy sites (0.7 kcal/mol) interacts with (*S*)-warfarin, most probably because of a larger number of contact points between the molecules of this enantiomer and the interacting sites. It has been shown that the formation of an inclusion complex combined with an interaction with the rim of the cyclodextrin cavities is generally needed for chiral recognition on cyclodextrin columns [8,14].

5. Conclusion

The retention process and the chiral recognition mechanism depend both strongly on the methanol–water ratio of the eluent. At low methanol content, the decrease of retention with increasing methanol content is entropically governed and the enantioselectivity for warfarin enantiomers is good. At high organic component content, the retention decrease is enthalpically driven and a fall of the enantioselectivity is observed.

The thermodynamic retention studies show that the retention behavior is mainly governed by hydrophobic interactions, with a mutual compensation between the entropic and enthalpic terms. In the reversed-phase mode on cyclodextrin stationary phases, the retention is explained by the formation of an inclusion complex, with the benzenic rings adsorbed inside the non-polar cyclodextrin cavities. Other interactions between the substituents of the warfarin chiral center and the polymeric linkers at the rim of the CD cavities explain the enantioselectivity. Both interactions are greatly affected by the hydrophobic environment at the interface between the solvent and the polymeric stationary phase.

References

[1] S.M. Han, D.W. Armstrong, in: A.M. Krstulovic (Ed.), Chiral Separation by HPLC – Applications to Pharmaceutical Compounds, Ellis Horwood, Chichester, 1989, p. 208.

[2] D.W. Armstrong, W. DeMond, B.P. Czech, Anal. Chem. 57 (1985) 481.
[3] K. Fujimura, S. Suzuki, K. Hayashi, S. Masuda, Anal. Chem. 62 (1990) 2198.
[4] N. Thuaud, B. Sébille, A. Deratani, G. Lelièvre, J. Chromatogr. 555 (1991) 53.
[5] N. Thuaud, B. Sébille, A. Deratani, B. Pöpping, C. Pellet, Chromatographia 36 (1993) 373.
[6] T. Cserháti, E. Forgács, J. Chromatogr. A 660 (1994) 313.
[7] E. Forgács, T. Cserháti, J. Chromatogr. A 668 (1994) 395.
[8] R.E. Boehm, D.E. Martire, D.W. Armstrong, Anal. Chem. 60 (1988) 522.
[9] Y. Matsui, T. Nishioka, T. Fujita, Topics Curr. Chem. 128 (1985) 61.
[10] M. Tanaka, T. Shono, D.Q. Zhu, Y. Kawaguchi, J. Chromatogr. 469 (1989) 429.
[11] A.M. Stalcup, S.C. Chang, D.W. Armstrong, J. Pitha, J. Chromatogr. 513 (1990) 181.
[12] D.W. Armstrong, C.D. Chang, S.H. Lee, J. Chromatogr. 539 (1991) 83.
[13] B. Sébille, N. Thuaud, J. Piquion, N. Béhar, J. Chromatogr. 409 (1987) 61.
[14] D.W. Armstrong, T.J. Ward, R.D. Armstrong, T.E. Beesley, Science 232 (1986) 1132.
[15] B.D. West, S. Preis, C.H. Schroeder, K.P. Luik, J. Am. Chem. Soc. 83 (1961) 2676.
[16] E. Renard, A. Deratani, G. Volet, B. Sébille, Eur. Polym. J. 33 (1997) 49.
[17] M. Guillaume, B. Sébille, Eur. Polym. J. 32 (1996) 19.
[18] J. Szejtli, Cyclodextrin Technology, Topics in Inclusion Science, Kluwer, 1988.
[19] E.J. Valente, E.C. Lingafelter, W.R. Porter, W.F. Trager, J. Med. Chem. 20 (1977) 1489.
[20] A. Jaulmes, C. Vidal-Madjar, Anal. Chem. 63 (1991) 1165.
[21] J.G. Dorsey, K.A. Dill, Chem. Rev. 89 (1989) 331.
[22] A. Alvárez-Zepeda, B.N. Barman, D.E. Martire, Anal. Chem. 64 (1992) 1978.
[23] B. Loun, D.S. Hage, Anal. Chem. 66 (1994) 3814.